

## EFFECTS OF THE MULTIPLE INTERNAL REFLECTION AND SAMPLE THICKNESS CHANGES ON DETERMINATION OF ELECTRO-OPTIC COEFFICIENT VALUES OF A POLYMER FILM

E. Nitiss <sup>a</sup>, M. Rutkis <sup>a</sup>, and M. Svilans <sup>b</sup>

<sup>a</sup> Institute of Solid State Physics, University of Latvia, Kengaraga 8, LV-1063 Riga, Latvia

<sup>b</sup> Faculty of Material Science and Applied Chemistry, Riga Technical University, Āzenes 14/24, LV-1048 Riga, Latvia

E-mail: edgars.nitiss@cfi.lu.lv

Received 8 September 2011; revised 18 January 2012; accepted 1 March 2012

New nonlinear optical (NLO) active organic materials are appealing candidates for optoelectronic and photonic technologies. For the evaluation of new NLO polymer materials for applicability in the mentioned technologies, the most important criteria are their electro-optic (EO) coefficients. We have implemented the Mach–Zehnder interferometric (MZI) method for the determination of EO coefficients of thin organic films. Despite the fact that other multiple optical methods for the determination of thin film EO coefficients are known, the MZI method has been chosen because this particular technique has high sensitivity to phase and intensity modulations in the sample arm of an interferometer and allows one to determine independently both thin film EO coefficients,  $r_{13}$  and  $r_{33}$ . In addition to the drawbacks described earlier we demonstrate that some other effects like electrostriction and multiple internal reflections in the sample have a considerable influence on light intensity at the MZI output. Taking into account these effects we have performed numerical simulations of the EO effect caused MZI output changes or modulation depth at different incidence angles using the Abeles matrix formalism. We can show that the modulated signal at the MZI output is highly dependent on the sample structure and is mainly governed by the effects mentioned above. For analysis of modulated signal components and determination of EO coefficients of a thin polymer film, a series of experiments was carried out on PMMA + DMABI 10 wt% samples.

**Keywords:** electro-optic coefficient, Mach–Zehnder interferometric method, nonlinear optical polymer, multiple internal reflections in polymer films

**PACS codes:** 81.70.Fy, 82.35.Ej

### 1. Introduction

Increasing interest has been devoted to new nonlinear optical (NLO) active organic materials due to their low cost, easy processability and potential applications as organic optical components in electro-optic (EO) devices.

Such organic EO materials are possible substitutes for traditional inorganic materials [1]. A high NLO activity is the most important material prerequisite for further successful application in EO devices making the evaluation of this property an important task for new material development.

Typically an organic EO material sample under investigation is a spin-coated thin film on an indium tin oxide (ITO) glass substrate and poled by an external electrical field. The EO performance of oriented film can be described by only two EO coefficients,  $r_{13}$  and  $r_{33}$  [2]. Several optical methods have been applied to characterise the EO performance of such organic materials [3–5]; however, some of the techniques are limited when it comes to determining  $r_{13}$  and  $r_{33}$  independently. In such cases, as  $r_{ef}$  is a function of  $r_{13}$  and  $r_{33}$ , the  $r_{33}/r_{13}$  ratio also needs to be known. Usually, if the film is poled at low poling fields ( $\mu E < kT$ ), this ratio is assumed to be constant and equal to 3 [6]. In

spite of high sensitivity to acoustic and mechanical vibrations, the Mach–Zehnder interferometric (MZI) techniques in the transmission or in the reflection mode are being applied more and more often [7, 8]. Researchers using the MZI technique in the transmission mode have mostly excluded multiple internal reflections and thickness change of the sample by electrostriction and piezoelectric effects from their considerations. To our knowledge, a limited number of investigators pay attention to these effects [9–11]; however, according to our observations, the effects can contribute greatly to the measured modulated signal amplitude and phase and therefore must be taken into account. For correct determination of both EO coefficients the light intensity and phase transmitted by the multilayer EO sample must be known. It can be described by the Abeles matrix formalism [12, 13]. In this contribution we would like to present the influence of the multiple internal reflection and sample thickness change effects on the determination of polymer film EO coefficients using the MZI technique.

### 2. Experimental set-up

The MZI set-up for EO measurements can be seen in Fig. 1. The sample was usually examined in the transmission configuration. In contrast to the reflection configuration, where the sample is used

as a mirror in the sample arm, here we can obtain modulation amplitude values as a function of the light incidence angle.

In our optical scheme we used a Helium-Neon laser (632.8 nm) as a light source. Polarisation of incident light can be controlled by a half wave plate  $\lambda/2$ . Afterwards, light is split into sample  $I_s$  and reference  $I_r$  arms of a MZI by a 50/50 beam splitter. By means of a small angle glass wedge and a computer controllable translation stage in the reference arm the interference phase of  $I_r$  and  $I_s$  and thus the AC signal measurement point can be shifted. To obtain an interference pattern the light of the reference and sample arms is combined by a second 50/50 beam splitter. The acquired interference pattern is detected by a large area Si photodiode. It is important to note that full overlapping of both light beams is necessary to achieve the maximum modulated signal. As the MZI is highly sensitive to any vibrations the elements of the optical set-up must be fixed firmly. An ultra stable beam splitter and mirror holders are suggested. A modulation voltage at 4 kHz was provided by a computer controlled lock-in detector (*Stanford Research Systems SR830*) and an amplifier (*Trek PZD350*). The light intensity modulation (AC signal) as well as the average MZI output light intensity (DC signal) was measured with the SR830 and recorded by the PC. It is important to note that the AC signal recovered by the Lock-in amplifier contains a notable fraction of crosstalk. This effect is caused by electromagnetic induction and can be recognised by its presence in the detection system with the laser light turned off. The crosstalk signal has the same frequency as the modulation caused by EO effect and creates an additional offset value in the signal detected by lock-in which is not dependent on MZI phase.

Typically, the polymer sample PMMA + DMA-BI 10 wt% (for a detailed molecular structure see Ref. [14]) used in this investigation was made by spin-coating (900 rpm speed, 300 rpm/s acceleration) it onto an ITO covered glass slide (*SPI Supplies ITO 70–100  $\Omega$* ) from a chloroform solution (concentration of 100 mg/ml) of appropriate amounts of components. The glass transition temperature of the polymer is approximately 110 °C.

There are two main possibilities how to obtain the sandwich sample structure. For sample 1, an ITO glass slide carrying the polymer is covered with another bare ITO glass slide as shown in Fig. 2,

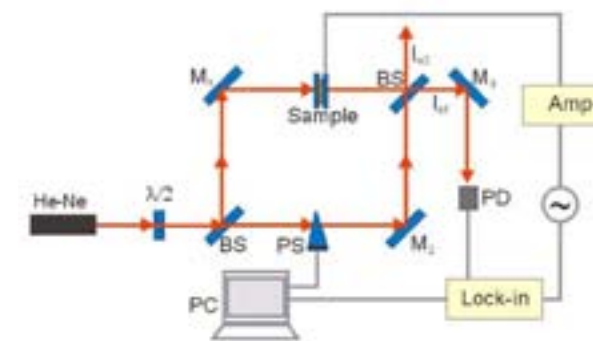


Fig.1. Experimental set-up of MZI for determination of EO coefficients of a thin organic film: helium-neon laser 632.8 nm *He-Ne*, half wave plate  $\lambda/2$ , beam splitter *BS*, mirrors  $M_1$ ,  $M_2$  and  $M_3$ , phase shifter *PS*, sample, photodiode *PD*, lock-in amplifier *Lock-in*, amplifier *Amp*, computer *PC*.

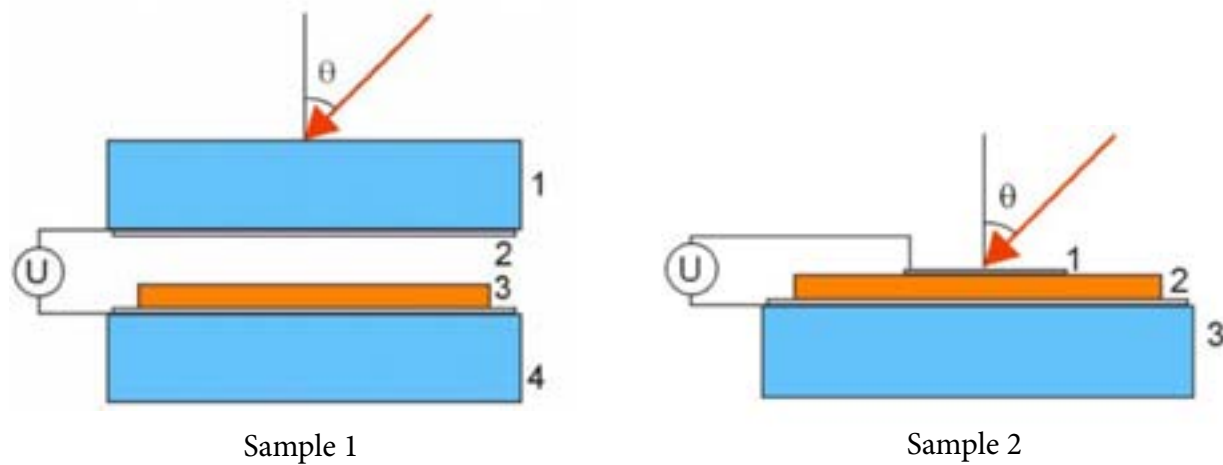


Fig. 2. Sample 1 geometry: 1, 4 ITO coated glass, 2 air gap, 3 PMMA + DMABI 10 wt%,  $\theta$  light incidence angle. Sample 2 geometry: 1 sputtered Al layer, 2 polymer (PMMA + DMABI 10 wt%), 3 ITO coated glass,  $\theta$  light incidence angle.

after which both slides are squeezed together in the sample holder. On a micron scale the surface of the sample, especially at slide edges, is rather rough. Due to this an air gap forms between the surface of polymer and second ITO electrode. Alternatively, for sample 2 an Al layer with the thickness of  $\sim 25$  nm can be sputtered directly onto the polymer as shown in Fig. 2. In this case the overall optical transmission coefficient of the sample is reduced; however, lower voltages on electrodes are necessary for material poling and observation of EO modulations.

The electrical connections to ITO electrodes were made using a silver paste. The *in situ* poling was performed at  $100^\circ\text{C}$  and  $80$  V on the electrodes

for 30 minutes for sample 1 and at  $100^\circ\text{C}$  and  $40$  V on the electrodes for 30 minutes for sample 2. The EO measurements were performed after at least 24 hours during which the charge relaxation had taken place. The parameters of the sandwich type samples are as shown in Table 1.

The thickness and refractive index of the polymer thin film was determined by a prism coupler (Metricon 2010), the extinction coefficient by measuring the absorption coefficient (Ocean Optics HR4000CG-UV-NIR). The air gap thickness was evaluated by interference fringe separation in the low absorbance part of the sample transmittance spectrum.

Table 1. Parameters of sandwich type samples.

Sample 1			
Layer	Thickness	Refractive index $n$ (at 632.8 nm)	Extinction coefficient $k$ (at 632.8 nm)
Glass	$1 \pm 0.02$ mm	1.50	0
ITO	15–30 nm	1.76	0
Air Gap	$5.95 \pm 2.38$ $\mu\text{m}$	1.00	0
Polymer	$0.90 \pm 0.09$ $\mu\text{m}$	1.54	$(10.4 \pm 0.01) \times 10^{-3}$
ITO	15–30 nm	1.76	0
Glass	$1 \pm 0.02$ mm	1.50	0
Sample 2			
Layer	Thickness	Refractive index $n$ (at 632.8 nm)	Extinction coefficient $k$ (at 632.8 nm)
Al layer	$25 \pm 1$ nm	1.45	7.54
Polymer	$1.21 \pm 0.09$ $\mu\text{m}$	1.54	$(10.4 \pm 0.01) \times 10^{-3}$
ITO	15–30 nm	1.76	0
Glass	$1 \pm 0.02$ mm	1.50	0

The EO experiment was performed as follows. Modulation voltage (typically  $50$  V rms for sample 1 and  $15$  V rms for sample 2) was applied to the electrodes, the output light intensity of MZI (DC signal) and the light modulation amplitude (AC signal) was detected with the Si photodiode and measured by the lock-in detector. Data was collected for  $20$  s at several MZI interference phase points and then averaged. The measurement series was done with *s* and *p* polarised light at several incident angles. Figure 3 shows typical measurement results where the interference phase is scanned with the motor-controlled glass wedge.

From Fig. 3 the maximal modulation depth  $m_{\text{max}}$  is calculated by

$$m_{\text{max}} = \frac{I_{\text{ac max}} - I_{\text{ac min}}}{(I_{\text{max}} - I_{\text{min}})}, \quad (1)$$

where  $I_{\text{ac max}}$  and  $I_{\text{ac min}}$  are the AC maximal and minimal modulated signal amplitudes,  $I_{\text{max}}$  and  $I_{\text{min}}$  are the maximal and minimal values of DC signal obtained from the MZI phase scan. The

maximal modulation depth is a dimensionless number used to describe the relative AC modulation intensity.

### 2.1. Description of the MZI output

The EO coefficient tensor  $r_{ijk}$  characterises the ability of a material to change its refractive index  $n$  when low frequency electric field  $E$  is applied:

$$\left(\frac{1}{\Delta n^2}\right) = \sum_k r_{ijk} E_k. \quad (2)$$

Due to Kleinman symmetry,  $r_{ijk}$  can be rewritten as  $r_{ijl}$  which is a  $6 \times 3$  tensor. In a poled polymer with point group symmetry of  $C_{\infty v}$  the effective EO coefficient can be rewritten for *s* polarised light as [15]

$$r_{\text{ef}} = r_{13} \quad (3a)$$

and for *p* polarised light as

$$r_{\text{ef}} = r_{13} \cos^2 \alpha + r_{33} \sin^2 \alpha, \quad (3b)$$

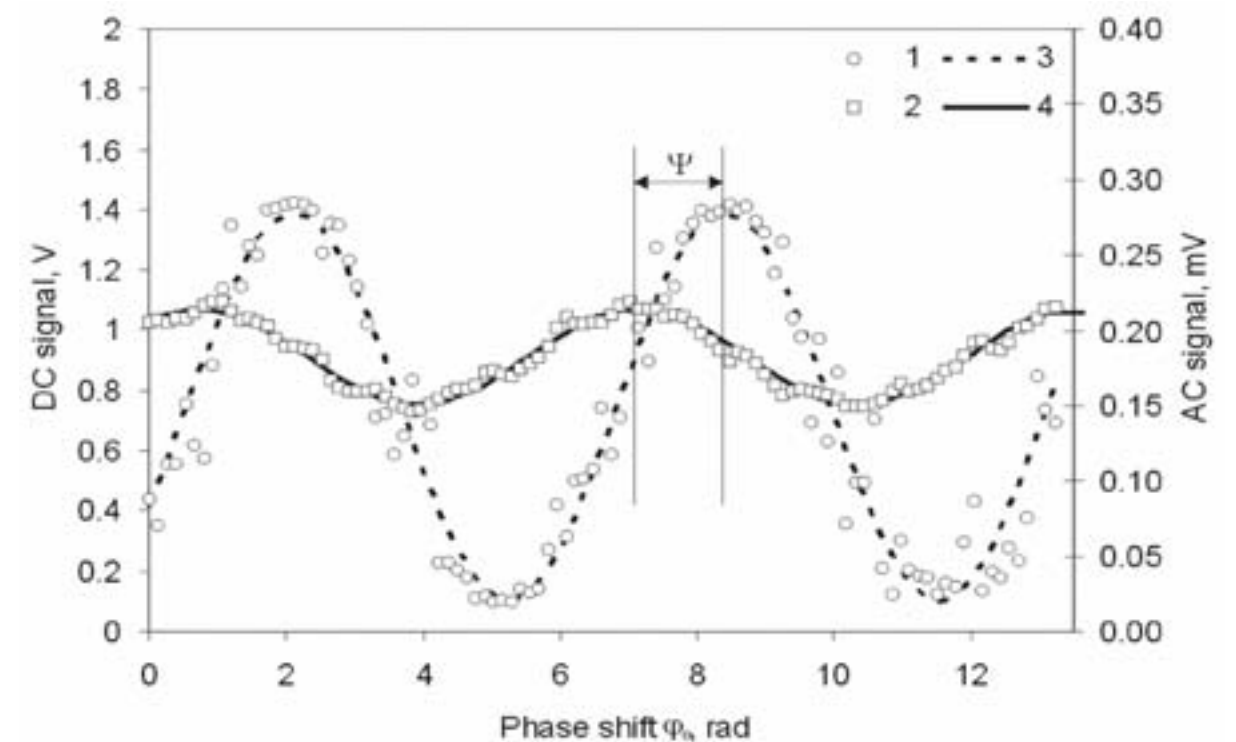


Fig. 3. Typical EO measurement performed at  $8^\circ$  incidence angle and *s* polarised light: 1  $I_{\text{DC}}$  signal experimental data, 2  $I_{\text{AC}}$  signal experimental data, 3  $I_{\text{DC}}$  signal sin approximation, 4  $I_{\text{AC}}$  signal sin approximation;  $\Psi$  is AC and DC signal maxima phase difference.

where  $r_{13}$  and  $r_{33}$  are the EO coefficients, and  $\alpha$  is the angle between the sample normal and light propagation direction.

The light intensity at the MZI output can be described by the two beam interference equation:

$$I_{01} = \frac{1}{2} \left[ I_r + TI_s + 2\sqrt{I_r TI_s} \cos(\varphi_0 + \varphi) \right], \quad (4)$$

where  $I_r$  is light intensity in the reference arm,  $I_s$  is light intensity in the sample arm without the sample,  $\varphi_0$  is interference phase difference (adjustable by phase shifter),  $T$  is transmission coefficient of the sample,  $\varphi$  is additional phase difference caused by the sample.

If an AC electrical field is applied to the sample the transmission  $T$  and phase  $\varphi$  are also modulated as affected by several parameters, e. g. the refractive index, light polarisation, sample thickness etc., with corresponding changes in the detected output light intensity and therefore the AC signal amplitude. Some parameters, e. g. thicknesses and complex refraction indices for each layer could be obtained from independent experiments. The unknown is the effective coefficient  $r_{ef}$  of EO active layer that we would like to determine from our MZI experiment. To describe the intensity and phase of light transmitted through the sample at a certain applied voltage one can use the Abelès matrix formalism [16].

### 3. Results and discussion

According to our observations, for sample 1 the maximal modulation depth  $m_{max}$  decreases as the incidence angle is increased. This dependence could not be explained just by multiple internal reflection effects. To describe experimental data adequately, sample thickness modulations needed to be included in our model. Thickness change can be caused by electrostriction or piezoelectric effects. To prove the existence of these effects and evaluate the magnitude of sample thickness modulation we used the MZI method in the reflection configuration [10]. In this case the ITO glass slide covered by a spin coated polymer thin film ( $\sim 1 \mu\text{m}$ ) was not enclosed by another slide, but a reflective 100 nm thick Al layer was deposited on the polymer. Then one of the mirrors ( $M_2$ , see Fig. 1) in our MZI set-up was replaced

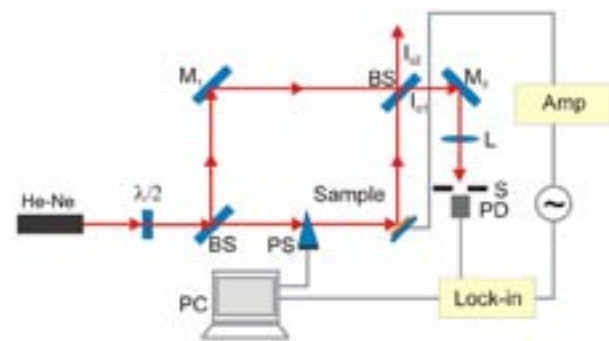


Fig. 4. Experimental set-up of MZI in reflection configuration for determination of a thin organic film thickness changes: helium-neon laser 632.8 nm *He-Ne*, half wave plate  $\lambda/2$ , beam splitter *BS*, mirrors  $M_1$  and  $M_2$ , phase shifter *PS*, sample, photodiode *PD*, lock-in amplifier *Lock-in*, amplifier *Amp*, computer *PC*.

by the sample with the Al layer facing the incident beam (see Fig. 4). The Al layer was thicker than for sample 2 so that light would not penetrate into the sample. In this configuration, when voltage is applied to electrodes, electric field can cause sample thickness changes, thereby changing the position of Al mirror surface and thus mechanically altering the optical path length in the sample arm of the MZI. To evaluate the actual thickness change of the sample the modulation depth equation is modelled for phase modulation only due to changes in the sample arm path length. In this case the average light intensity at the MZI output, or DC signal, has a phase difference of  $\pi/2$  with respect to the 4 kHz AC modulated signal amplitude since the beam intensities in both arms,  $I_r$  and  $I_s$ , remain constant.

For a modulation depth (Eq. (1)) of  $7 \times 10^{-5}$ , which is the maximal measured modulation depth of an unpoled sample, the sample thickness alteration of approximately 14 pm was estimated. In Fig. 5 we present the modulation depth determined according to Eq. (1) as a function of applied modulation voltage. The maximal modulation depth dependence on modulation voltage exhibits a quadratic and a linear component caused by electrostriction and piezoelectric effects, respectively. Moreover, both of these effects are more pronounced for the poled polymer films.

In Fig. 6 the maximal modulation depth of sample 1 (see Table 1) at different light incidence

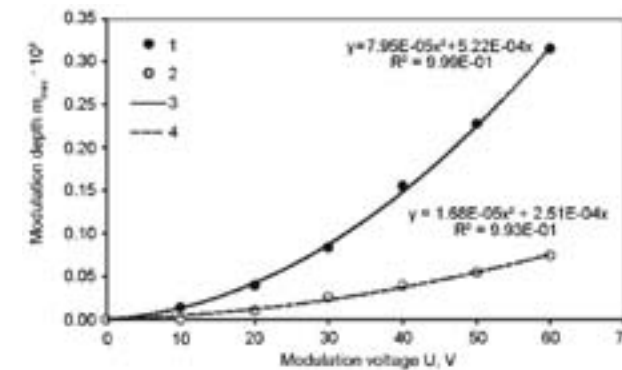


Fig. 5. Modulation depth  $m_{max}$  as a function of modulation voltage  $U$  for a MZI in the reflection configuration. Quadratic function regression is applied: 1 modulation depth  $m_{max}$  of poled film, 2 modulation depth  $m_{max}$  of unpoled film, 3 quadratic approximation of modulation depth  $m_{max}$  of poled film, 4 quadratic approximation of modulation depth  $m_{max}$  of unpoled film.

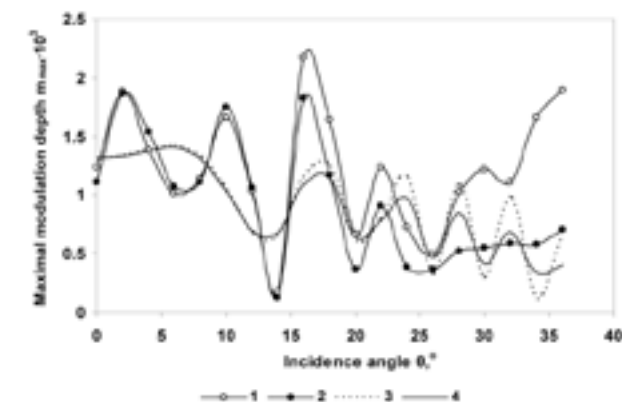


Fig. 6. Modulation depth dependence on the incidence angle in MZI in the transmission configuration for sample 1: 1, 2 experimental data for *s* and *p* polarised light, respectively; 3, 4 numerical approximation with MatLab performed using functions based on Abeles matrix formalism.

angles is shown. The measurement is performed by MZI in the transmission configuration by applying 50 V rms on the sample. The most important thing to notice in Fig. 6 is that the maximal modulation depth of *s* polarised light is higher than of *p* polarised light. From Eqs. (3a) and (3b) we would expect the refractive index change and therefore the maximal modulation depth for *p* polarised light to be higher as the effective EO coefficient is a combi-

nation of both  $r_{13}$  and  $r_{33}$ . In case of *s* polarised light the modulation depth should be dependent only on  $r_{13}$ . However, due to electrostriction and piezoelectric effect the sample thickness changes take place in addition to refractive index changes so that both the light phase and the amplitude are modulated causing the modulation depth decrease for greater incidence angles. The modelling is performed by refining the preliminary experimental results of a thin film and air gap thicknesses and varying the EO coefficients  $r_{13}$  and  $r_{33}$  and sample thickness alteration  $\Delta l$  due to electrostriction and piezoelectric effects.

For approximation of sample 1 experimental data we used a simple ITO-polymer-air gap-ITO layer system (Fig. 2 and Table 1) and glass as input and output media. This approach neglects interference effects caused by multiple light reflections within the glass slides and therefore theoretical lines are much smoother than experimental. Of course we could take into account glass slides as additional layers in our approximation. In that case noise-like interference fringes are superposed on the curves. The angular spacing of these fringes is well below the experimental incidence angle resolution. After performing the first numerical approximations for sample 1 we found that the modulation depth is a linear combination of NLO active layer thickness and EO modulations. When the EO coefficients were calculated taking into account a thickness modulation amplitude in the range of several tens of pm, the obtained  $r_{33}$  to  $r_{13}$  ratio  $\sim 10$  and  $r_{33}$  value close to 100 pm/V were obviously too high. The ratio of  $r_{33}$  to  $r_{13}$  can be estimated by measuring the ratio of NLO coefficients  $d_{33}$  and  $d_{13}$ . Both EO and NLO coefficients characterise the material nonlinearity and are proportional to the second order polarisability  $\chi^{(2)}$ , but are used to describe the nonlinearity at different interactions and conditions. The NLO coefficient ratio  $d_{33}/d_{13}$  (nominally the same as  $r_{33}/r_{13}$  [17]) measurements performed by the second harmonic generation Maker fringe technique on the same sample yielded a value of 1.86. This suggests that the modulation is mainly caused by some effect other than EO variations. As described above the modulations could be caused by thickness changes in the polymer layer. The air gap (Fig. 2) thickness modulations can also take place as shown previously [18]. Therefore, the final modelling was performed allowing only air gap and NLO active layer thickness modulations  $\Delta l_{air}$  and

$\Delta l$ , respectively. As it turned out in such case the calculated modulation depth was in good agreement with experimental data. The experimental data and best fit are shown in Fig. 6. The approximation values are shown in Table 2.

Table 2. Sample 1 parameters calculated from numerical approximation results.

Parameter	Value
Thickness $l$	$0.85 \pm 0.05 \mu\text{m}$
Air gap	$5.85 \pm 0.10 \mu\text{m}$
$\Delta l_{\text{air}}$	$170 \pm 5 \text{ pm}$
$\Delta l$	$76.5 \pm 1.0 \text{ pm}$

From comparison of data in Tables 1 and 2 one can see that the sample (polymer film) and air gap thicknesses are in good agreement with the preliminary experimental results. As expected, with thickness changes of air gap and NLO active layer, one can have a good approximation of modulation depth values.

The dependence of modulation depth on the incidence angle for sample 2 can be seen in Fig. 7. After measuring the dependence of modulation depth on the applied voltage we found that the dependence was linear. As thickness changes in the sample were expected to be quadratic, we consider that the

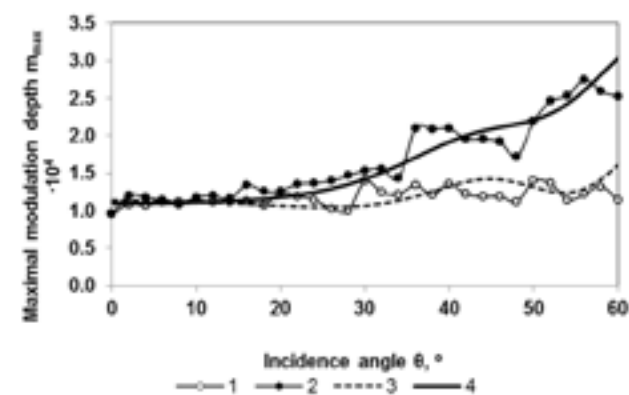


Fig. 7. Modulation depth dependence on the incidence angle in MZI in the transmission configuration for sample 2: 1, 2 experimental data for  $s$  and  $p$  polarised light, respectively; 3, 4 numerical approximation with MatLab performed using functions based on the Abeles matrix formalism.

effect of thickness change in this case has a small influence on the total modulation depth. Therefore, we excluded the sample thickness change effect in approximation by leaving only EO modulations. The approximation can be seen in Fig. 7. The numerical fit values can be seen in Table 3.

Table 3. Sample 2 parameters calculated from numerical approximation results.

Parameter	Value
Thickness $l$	$1.34 \pm 0.05 \mu\text{m}$
$r_{13}$	$0.19 \pm 0.02 \text{ pm/V}$
$r_{33}$	$0.55 \pm 0.06 \text{ pm/V}$

#### 4. Conclusions

Both EO coefficients ( $r_{13}$  and  $r_{33}$ ) of poled polymer films can be determined by applying the Abeles matrix formalism for numerical approximation of experimental MZI data at different incidence angles. However, one has to consider the sample structure. If an air gap is formed in the sample, the modulated signal in the MZI is usually generated by the air gap thickness modulations. The thickness modulations in the NLO active layer are also to be taken into account. An experimental procedure and data modelling are demonstrated for determining the EO coefficients of a poled PMMA + DMABI 10 wt% thin film. The obtained values are  $r_{13} = 0.19 \pm 0.02 \text{ pm/V}$  and  $r_{33} = 0.55 \pm 0.06 \text{ pm/V}$ .

#### Acknowledgements

This research was granted by ERDF 2.1.1.1 activity project No. 2010/0308/2DP/2.1.1.1.0/10/APIA/VIAA/051 “Development of Polymer EO Modulator Prototype Device” and Latvian National Research Program “Development of Innovative Multifunctional Materials, Signal Processing and Information Technologies for Competitive Science Intensive Products”.

#### References

- [1] L.R. Dalton, Rational design of organic electro-optic materials, *J. Phys. Condens. Matter* **15**, 897–934 (2003).
- [2] A. Knoesen, M.E. Molau, D.R. Yankelevich, M.A. Mortazavi, and A. Dienes, Corona-poled

nonlinear polymeric films: in situ electric field measurement, characterization and ultrashort-puls applications, *Int. J. Nonlinear Opt. Phys.* **1**(1), 73–102 (1992).

- [3] M. Aillerie and N. Theofanous, Measurement of the electro-optic coefficients: description and comparison of the experimental techniques, *Appl. Phys. B* **70**, 317–334 (2000).
- [4] C.C. Teng and H.T. Man, Simple reflection technique for measuring the electro-optic coefficient of poled polymer films, *Appl. Phys. Lett.* **56**(18), 1734–1737 (1990).
- [5] W.H.G. Horsthuis and G.J.M. Krijnen, Simple measuring method for electro-optical coefficients in poled polymer waveguides, *Appl. Phys. Lett.* **55**(7), 616–618 (1989).
- [6] C. Maertens, C. Detrembleur, P. Dubois, R. Jérôme, R. Blanche, Ph.C. Lemaire, Synthesis and electrooptic properties of a new chromophore dispersed or grafted in a carbazolyl methacrylate matrix, *Chem. Mater.* **10**, 1010–1016 (1998).
- [7] M. Sigelle and R. Hierle, Determination of electrooptic coefficients of 3-methyl 4-nitropyridine 1-oxide by an interferometric phase-modulation technique, *J. Appl. Phys.* **52**(6), 4199–4204 (1981).
- [8] M.J. Shin, H.R. Cho, J.H. Kim, S.H. Han, and J.W. Wu, Optical interferometric measurement of the electro-optic coefficient in nonlinear optical polymer films, *J. Korean Phys. Soc.* **31**(1), 99–103 (1997).
- [9] R. Meyrueix and O. Lemonnier, Piezoelectrically induced electrooptical effect and dipole orientation measurement in undoped amorphous polymers, *J. Phys. D: Appl. Phys.* **27**, 379–386 (1994).
- [10] C. Greenlee, A. Guilmo, A. Opadeyi, R. Himmelhuber, R.A. Norwood, M. Fallahi, J. Luo, S. Huang, X.H. Zhou, A.K.Y. Jen, and N. Peyghambarian, Mach-Zehnder interferometry method for decoupling electro-optic and piezoelectric tensor components in poled polymer films, *Proc. SPIE* **7774**, 77740D–2 (2010).
- [11] F. Qui, X. Cheng, K. Misawa, and T. Kobayashi, Multiple reflection correction in the determination of the complex electro-optic constant using a Mach-Zehnder interferometer, *Chem. Phys. Lett.* **266**, 153–160 (1997).
- [12] P. Nagtegaele, E. Brasselet, and J. Zyss, Anisotropy and dispersion of a Pockels tensor: a benchmark for electro-optic organic thin-film assessment, *J. Opt. Soc. Am. B* **20**(9), 1932–1936 (2003).
- [13] F. Abelès, La détermination de l'indice et de l'épaisseur des couches minces transparentes, *J. Phys. Radium* **11**(7), 310–314 (1950).
- [14] M. Rutkis, A. Vembris, V. Zauls, A. Tokmakovs, E. Fonavs, A. Jurgis, and V. Kampars, Novel second-order nonlinear optical polymer materials containing indandione derivatives as a chromophore, *Proc. SPIE* **6192**, 61922Q (2006).
- [15] R.A. Norwood, M.G. Kuzyk, and R.A. Keosian, Electro-optic tensor ratio determination of side chain copolymers with electro-optic interferometry, *J. Appl. Phys.* **75**(4), 1869–1874 (1994).
- [16] S. Larouche and L. Martinu, OpenFilters: open-source software for design, optimization, and synthesis of optical filters, *Appl. Opt.* **47**(13), C219–C230 (2008).
- [17] O. Ahumada, C. Weder, P. Neuenschwander, and U.W. Suter, Electro-optical properties of waveguides based on a main-chain nonlinear-optical polyamide, *Macromolecules* **30**, 3256–3261 (1997).
- [18] E. Nitiss, M. Rutkis, and O. Vilitis, Determination of electro-optic coefficient of thin organic films by Mach-Zehnder interferometric method, *Latv. J. Phys. Tech. Sci.* **46**(3), 5–14 (2009).

## DAUGKARTINIO VIDINIO ATSPINDŽIO IR BANDINIO STORIO KITIMO ĮTAKA POLIMERINIO SLUOKSNIŲ ELEKTROOPTINIŲ KOEFICIENTŲ VERČIŲ NUSTATYMU

E. Nitišs<sup>a</sup>, M. Rutkis<sup>a</sup>, M. Svilans<sup>b</sup>

<sup>a</sup>Latvijos universiteto Kietojo kūno fizikos institutas, Ryga, Latvija

<sup>b</sup>Rygos technikos universiteto Medžiagotyros ir taikomosios chemijos fakultetas, Ryga, Latvija

### Santrauka

Naujos organinės netiesiškos optiškai aktyvios medžiagos yra naudojamos optoelektroniniuose ir fotoniuose taikymuose. Tokių medžiagų tinkamumas minėtiems taikymams gali būti vertinamas pagal jų elektrooptinius (EO) koeficientus. Mes pritaikėme Macho ir Cènderio (Mach–Zehnder, MZ) interferometrijos metodą plonų organinių sluoksnių EO koeficientams nustatyti. Nepaisant daugybės kitų EO koeficientų nustatymo ploniems sluoksniams optinių metodų, šį metodą pasirinkome todėl, kad jis pasižymi dideliu jautrumu fazės ir intensyvumo moduliacijoms interferometro bandinio petyje ir leidžia nepriklausomai matuoti abu plonojo sluoksnio EO koeficientus –  $r_{13}$  ir  $r_{33}$ .

Parodėme, kad elektrostrikcija ir daugkartiniai vidiniai atspindžiai bandinyje stipriai veikia šviesos intensyvumą MZ interferometro išėjime. Atsižvelgdami į šiuos reiškinius, skaitmeniškai naudodami Abelės matricų formalizmą, sumodeliavome EO koeficientų poveikį MZ interferometro signalo kaitai arba moduliacijos gylį esant skirtingiems kritimo kampams. Pavyko parodyti, kad moduluotas signalas MZ interferometro išėjime labai priklauso nuo bandinio sandaros ir yra stipriai lemiamas EO koeficientų. Moduluoto signalo sandų analizei ir plonų polimerinių sluoksnių EO koeficientų nustatymui atlikome keliolika eksperimentų su PMMA ir 10 svorio % DMABI bandiniais.